HV-MAPS
(High Voltage Monolithic Active Pixel Sensors)
for the PANDA Luminosity Detector

Tobias Weber for the PANDA collaboration
in collaboration with the Heidelberg Mu3e group

INSTR14
25.02.2014

PANDA Experiment

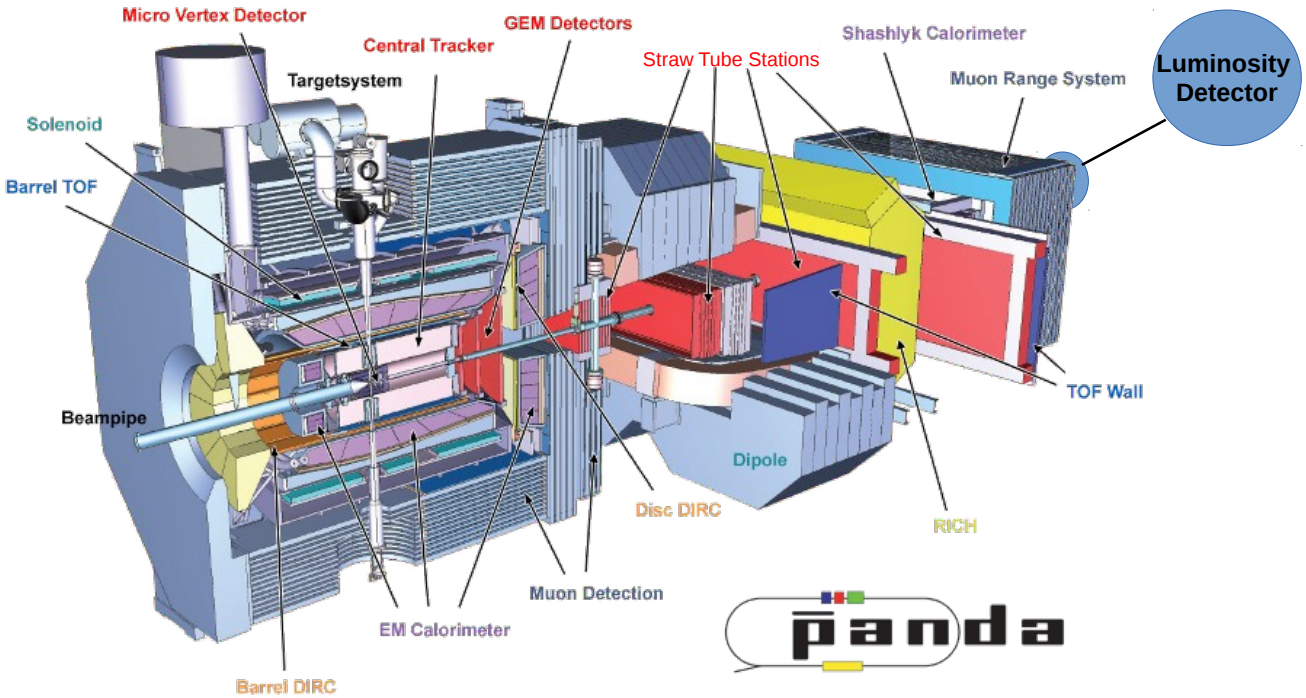

Physics Program

- hadron spectroscopy
- nucleon structure
- hyper nuclei
- hadrons in matter

PANDA Experiment

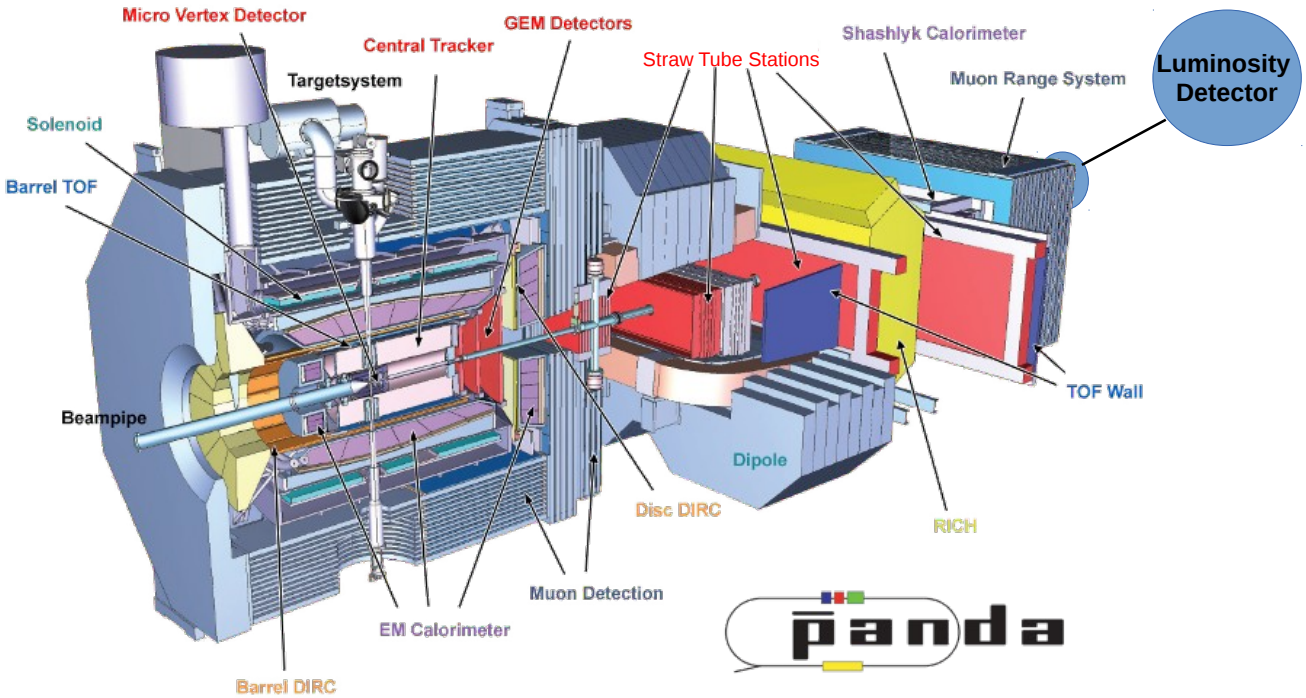

Measurements at PANDA

- $p\bar{p}$-formation experiments
  - resonance scans
  - threshold scans

PANDA Experiment

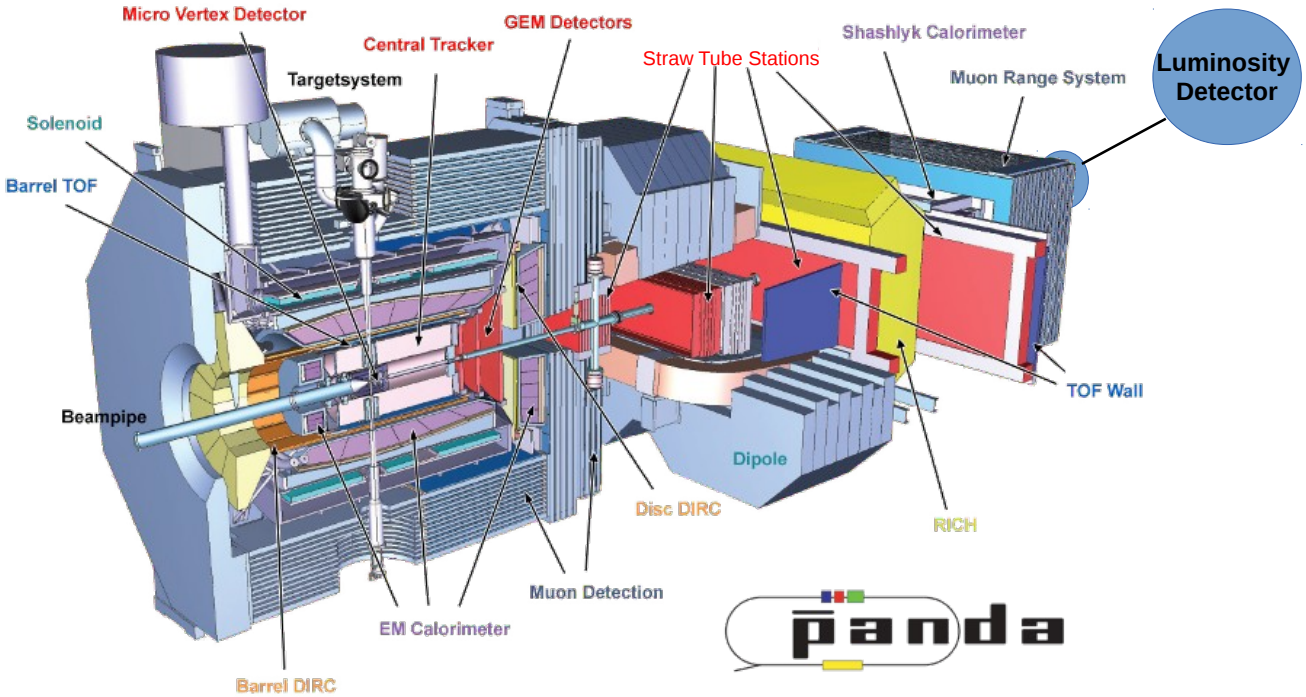

Measurements at PANDA

- $p\bar{p}$-formation experiments
- production experiments

PANDA Experiment

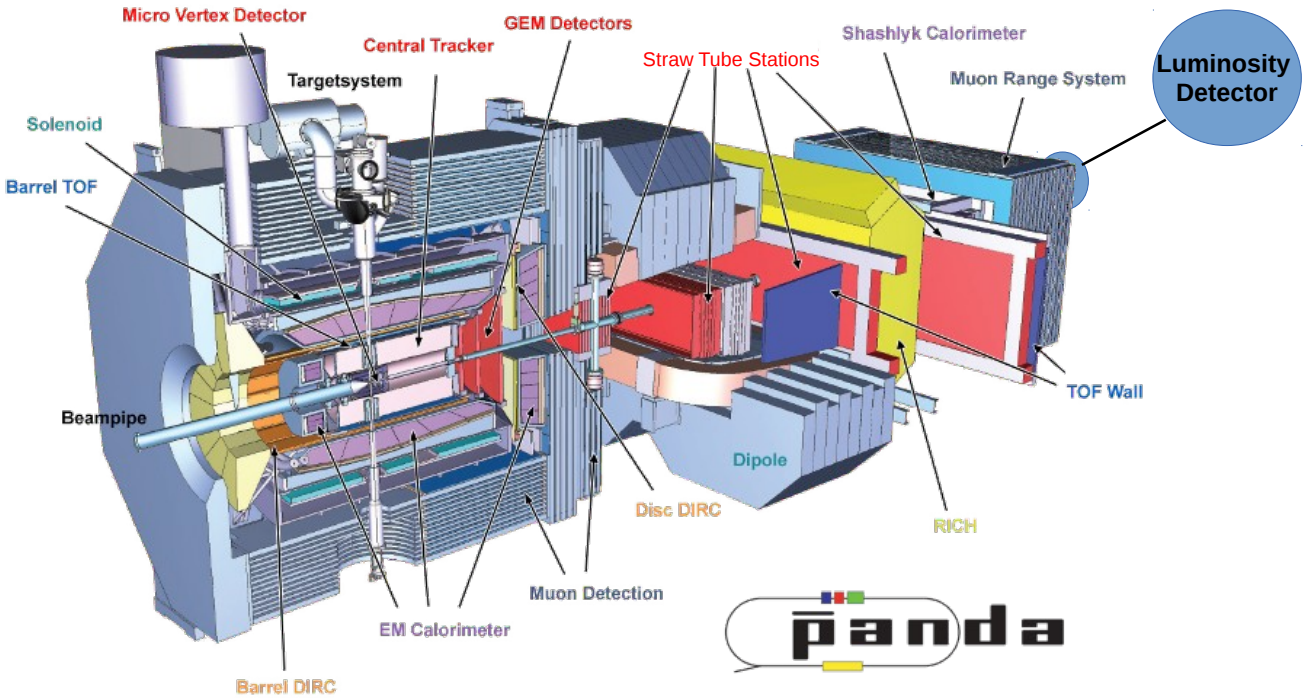

Measurements at PANDA

- $p\bar{p}$-formation experiments
- production experiments

$\Rightarrow$ luminosity measurement

Luminosity Detector

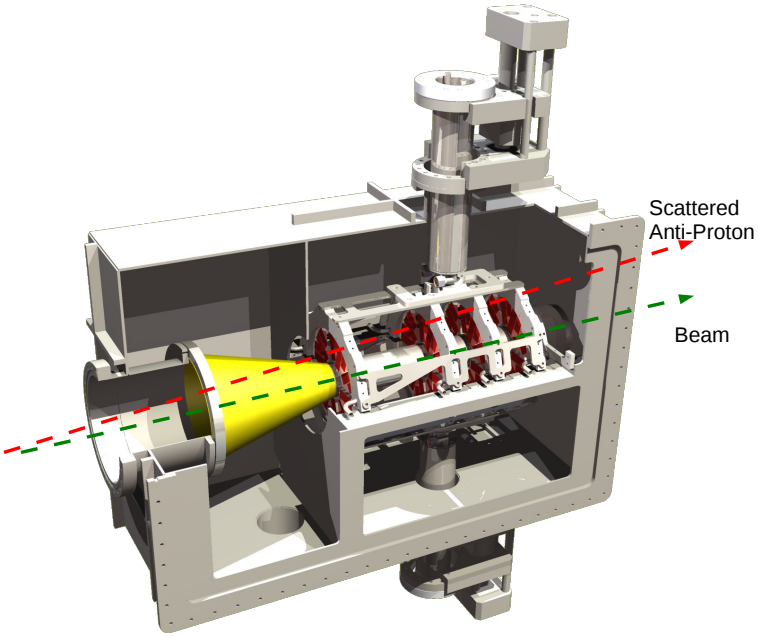

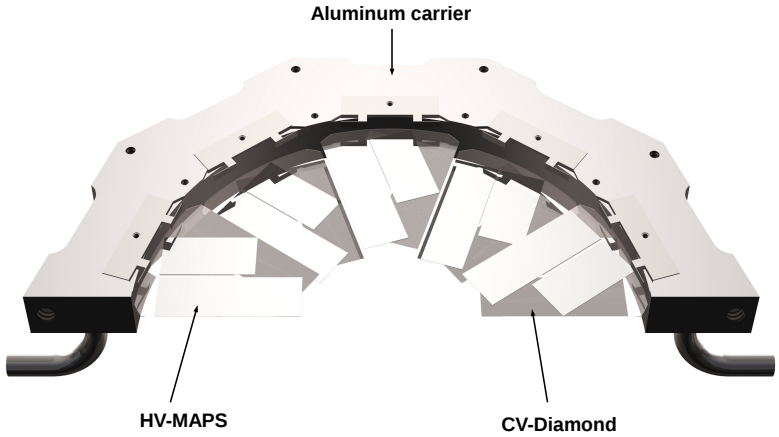

- reconstruction of angle of the elastically scattered antiprotons
- four silicon tracker stations
- 400 HV-MAPS in total

High Voltage Monolithic Active Pixel Sensors

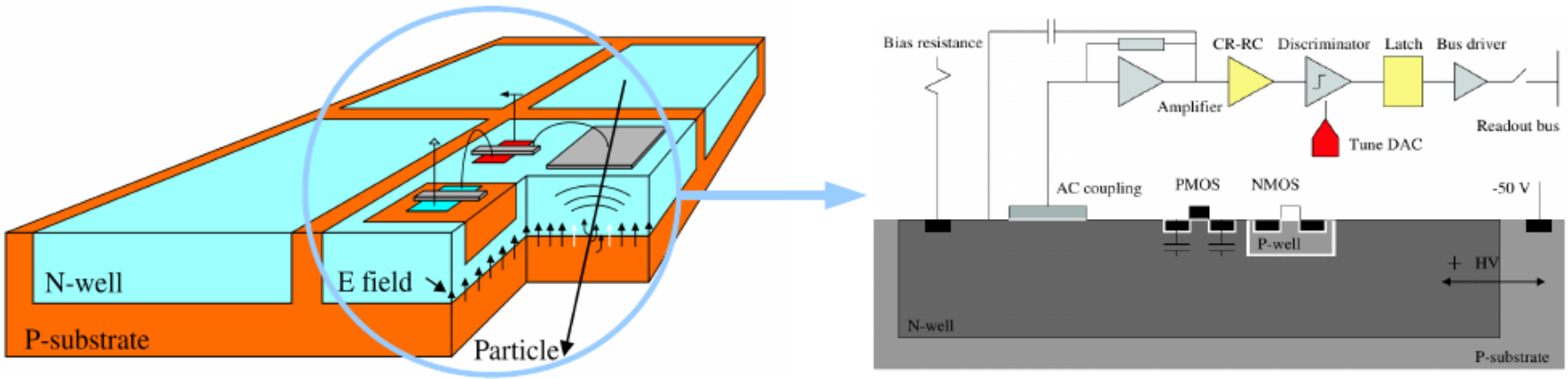

developed by Ivan Perić for the Mu3e Experiment

- 180 nm technology
- bias voltage (≈60V)
  - 14 µm depletion layer
  - fast charge collection
- radiation tolerant
- leading edge discriminator
- thinable to less than 50 µm

High Voltage Monolithic Active Pixel Sensors

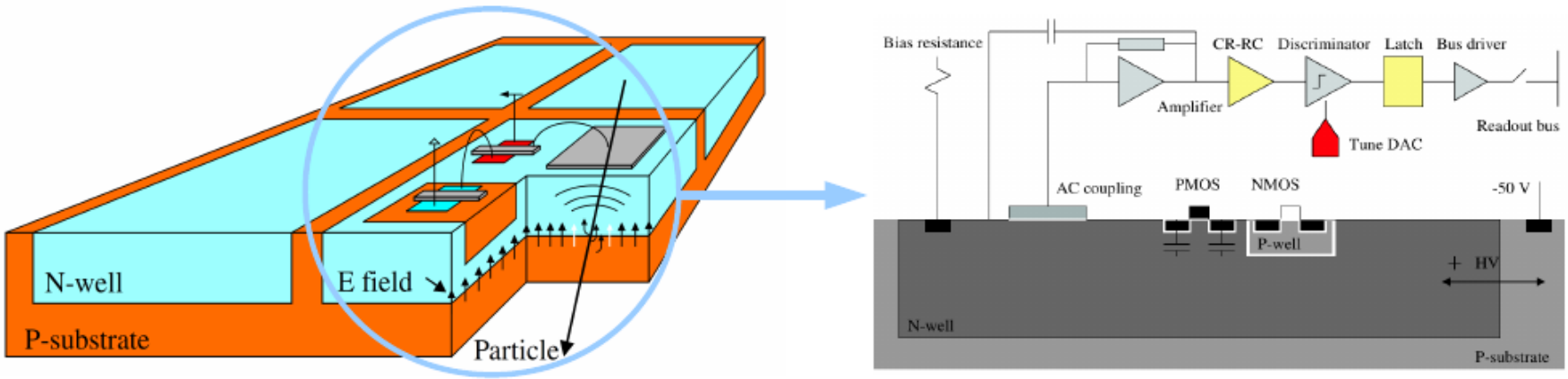

developed by Ivan Perić for the Mu3e Experiment

- size of 2x2 cm with 80x80 µm pixels
- digital part on one chip side, active area >90%
- readout frequency up to 40 MHz
- LVDS-Link @ 400-800 Mbps

High Voltage Monolithic Active Pixel Sensors

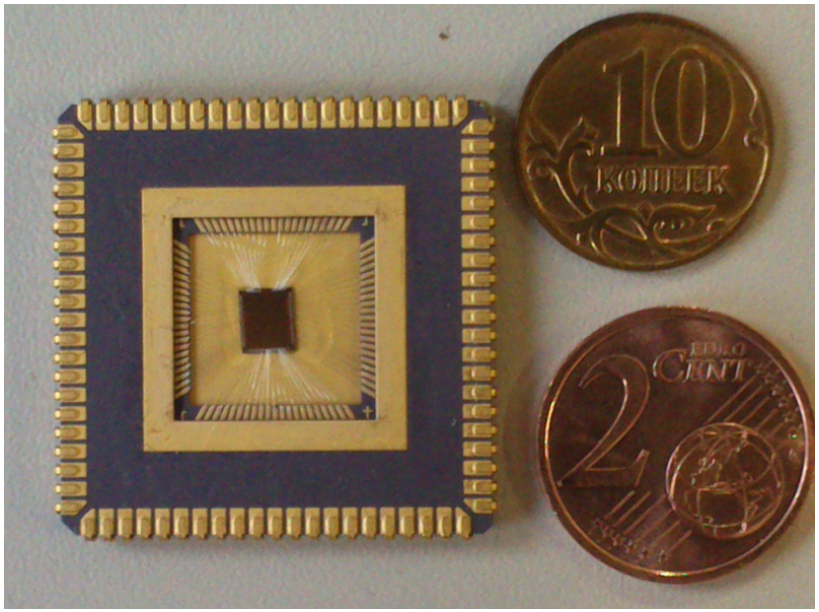

MuPix 4 Prototype

- 40x32 pixels with 80 µm x 92 µm
- column logic on chip
- parallel data readout (no serial link)
- readout and slow control by FPGA-Board

DESY Test Beam

Test Beam by Mu3e group with EUDET-telescope

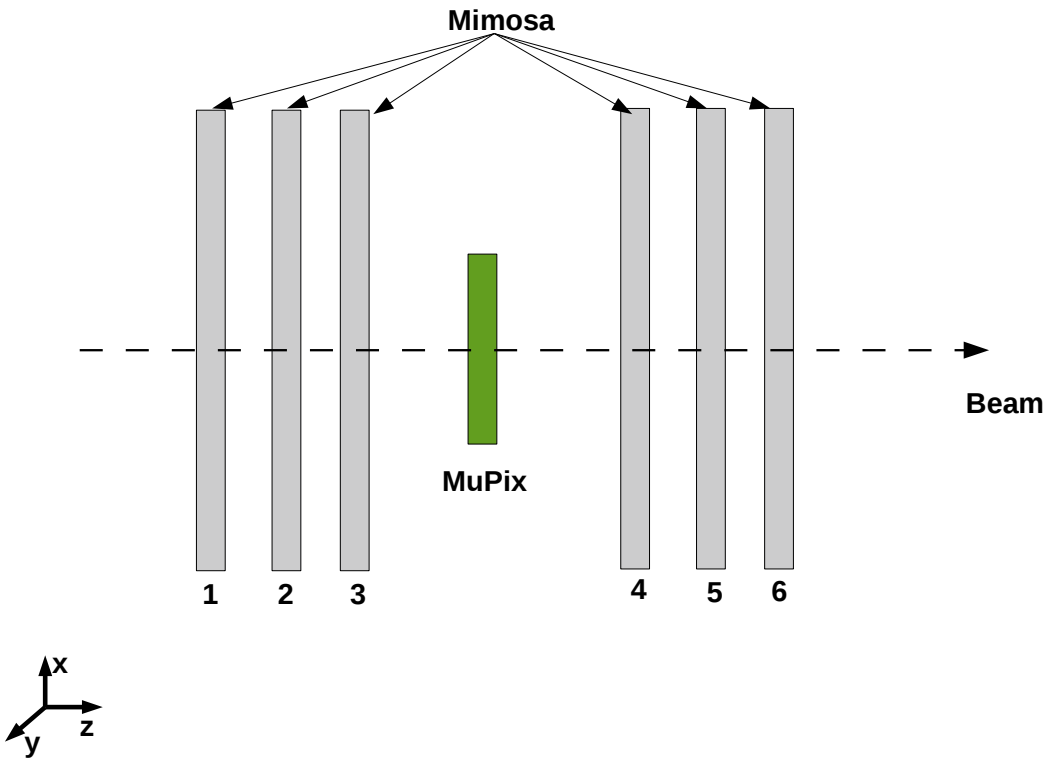

- electron beam with 3-5 GeV
- measurement of sensor efficiency

DESY Test Beam

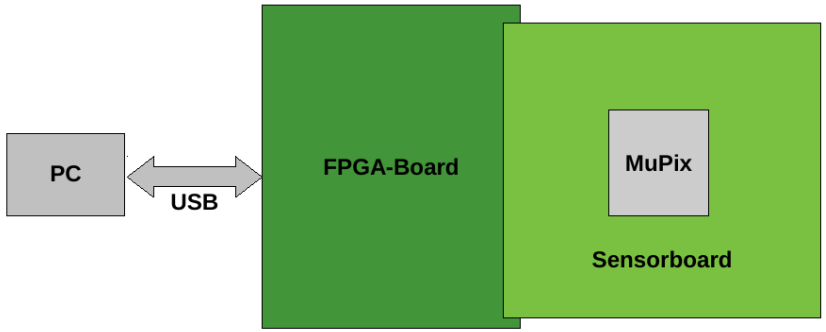

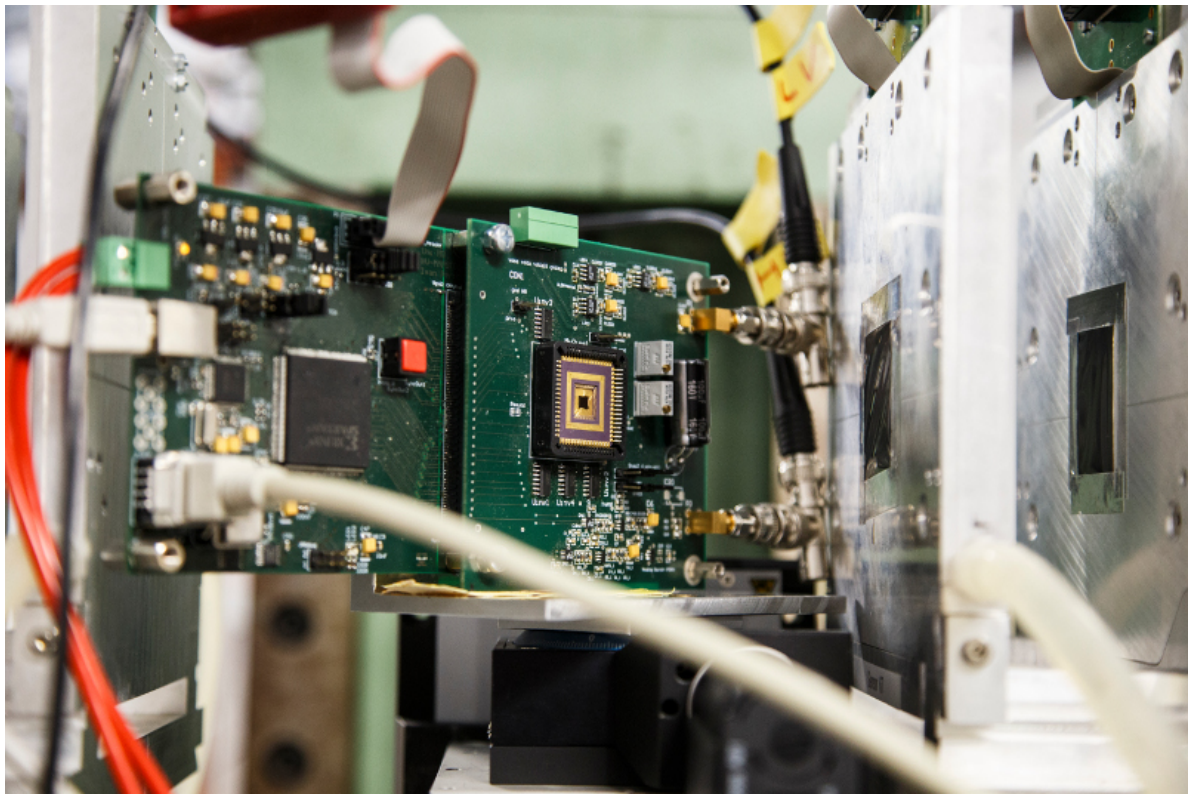

Eutel Telescope Software

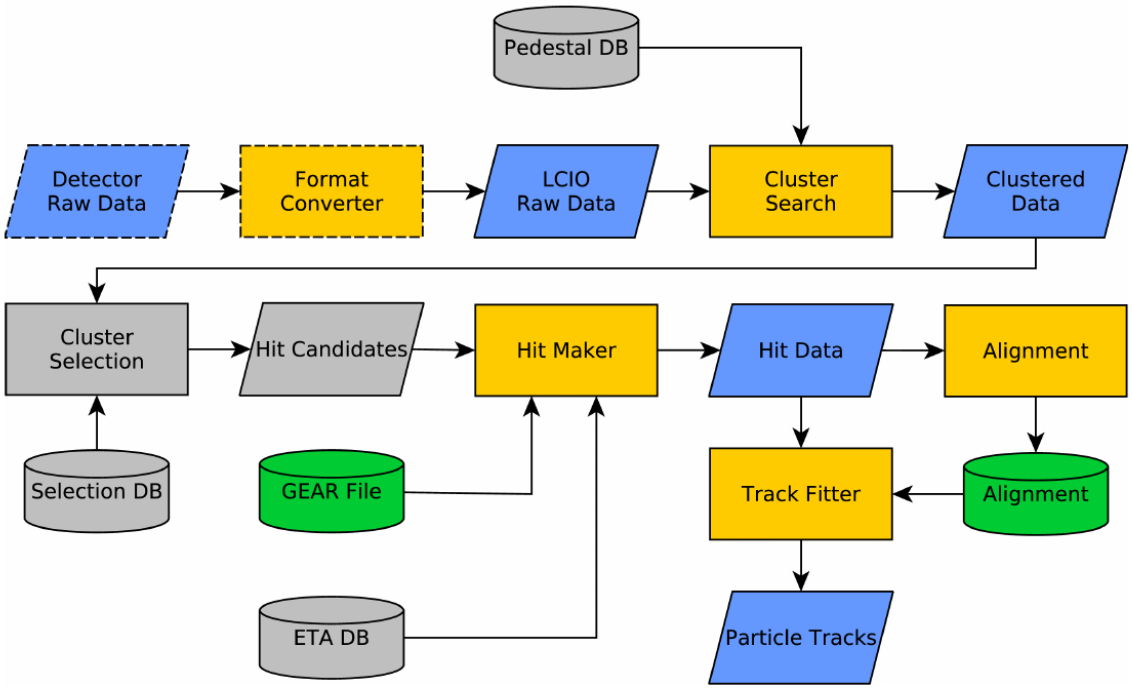

- reconstruction tool set for test beam
- based on ILC software

MuPix 4: A Hybrid Strixel

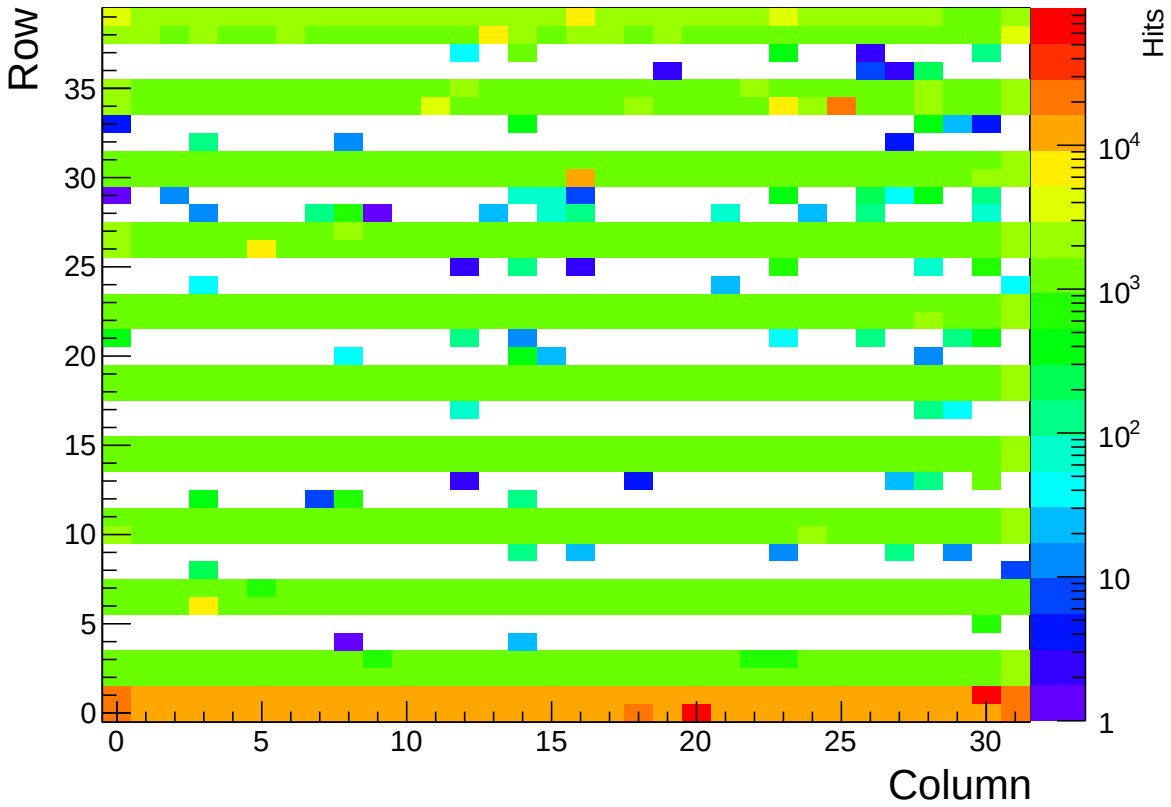

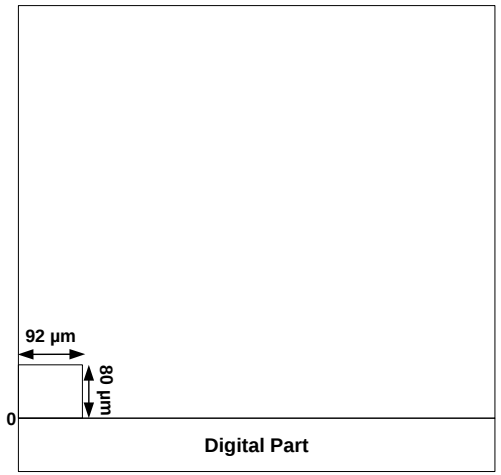

- timing problem in row address readout
  $\Rightarrow$ projection of hits into first two rows
- high noise in few pixels

Telescope Resolution and Alignment

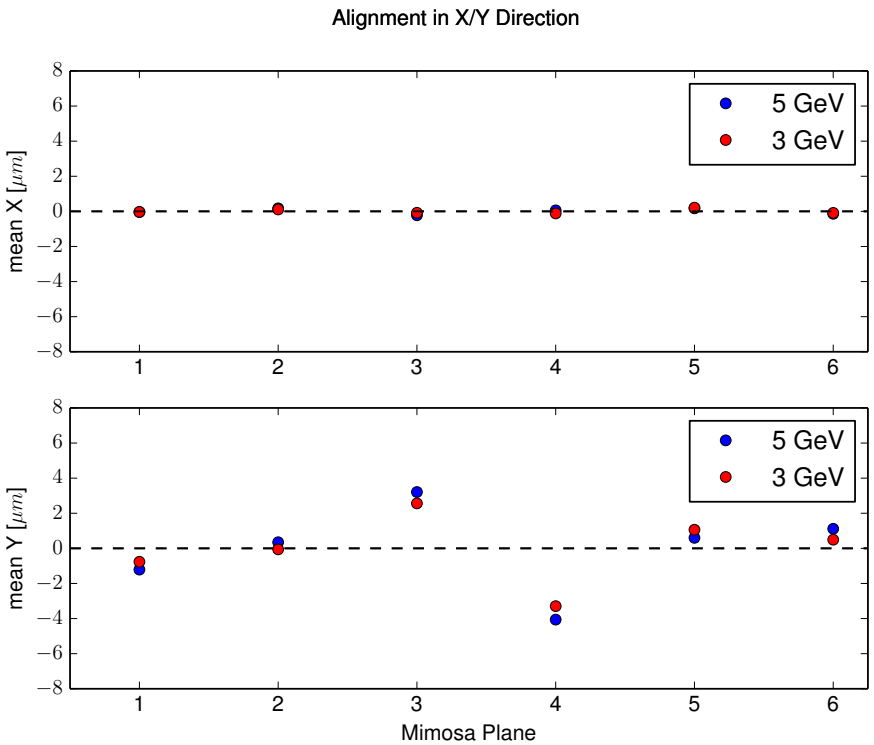

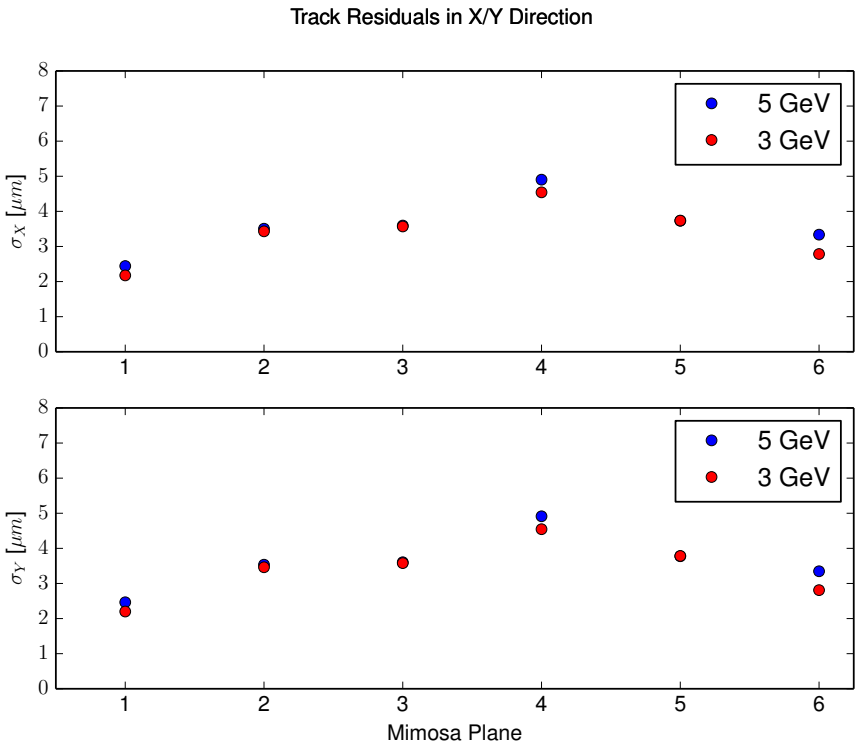

- good alignment in X direction
- offsets in Y direction on telescope planes next to MuPix
- track residuals below 6 µm

Matching Tracks to Hits

General Cuts

- removal of Hits/Tracks in broken rows
- ignore sensor edges

Hit-Track Matching

rectangular cut on hit-track distance $|d_i| < 0.95 \cdot \text{pitch}_i$

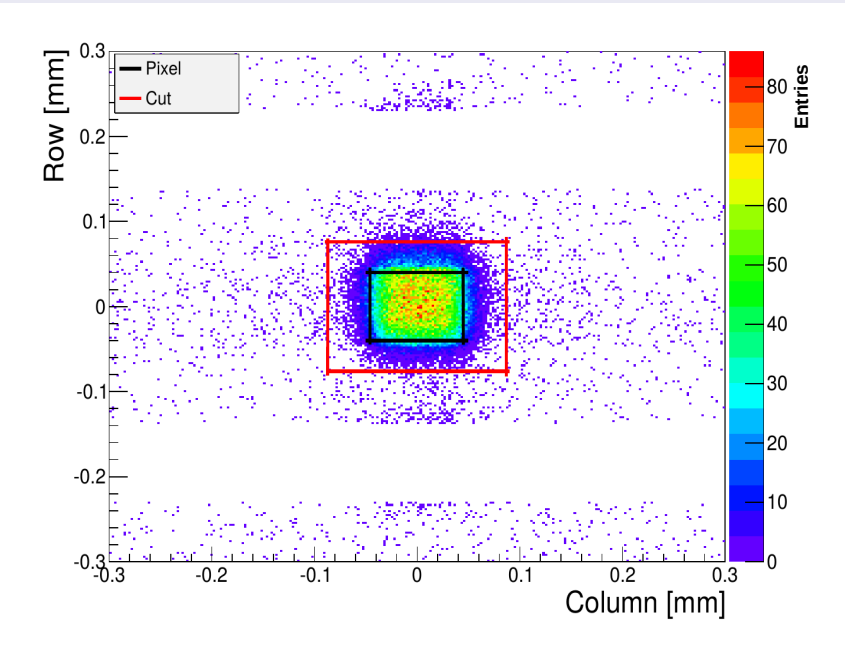

Global Efficiency

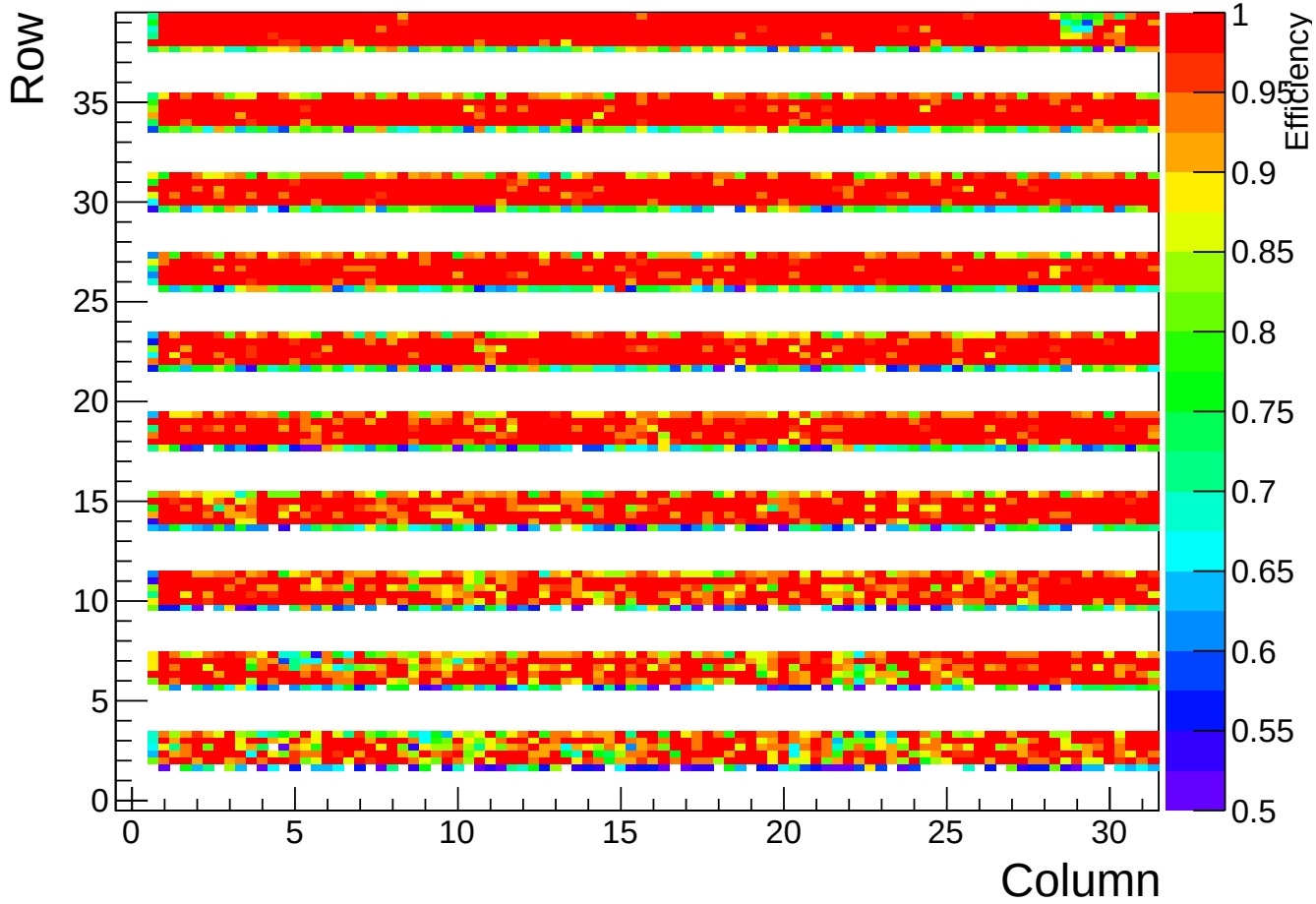

- efficiency up to 99%

Projected Efficiency

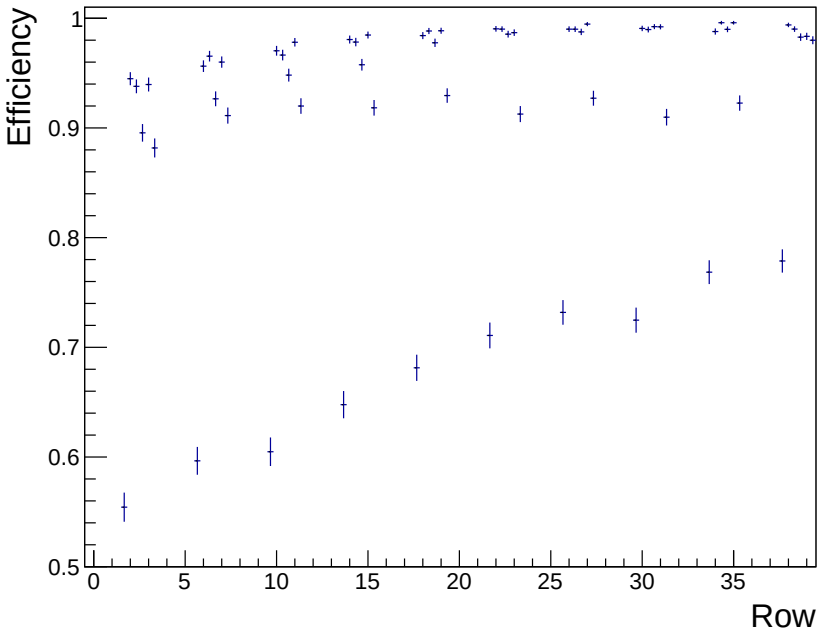

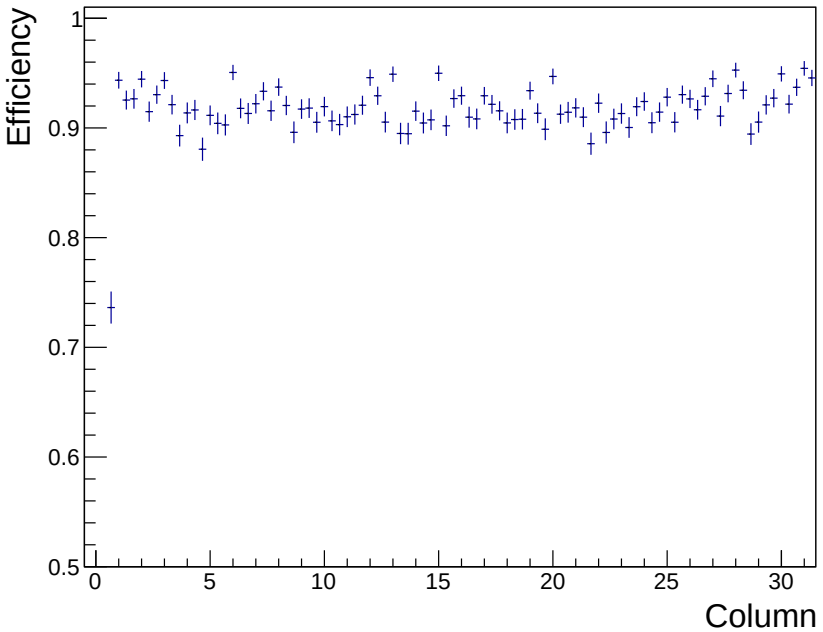

- increase of efficiency with row number
- row dependence probably caused by faulty TDAC settings
- average column efficiency above 95%

Sub-Pixel Efficiency

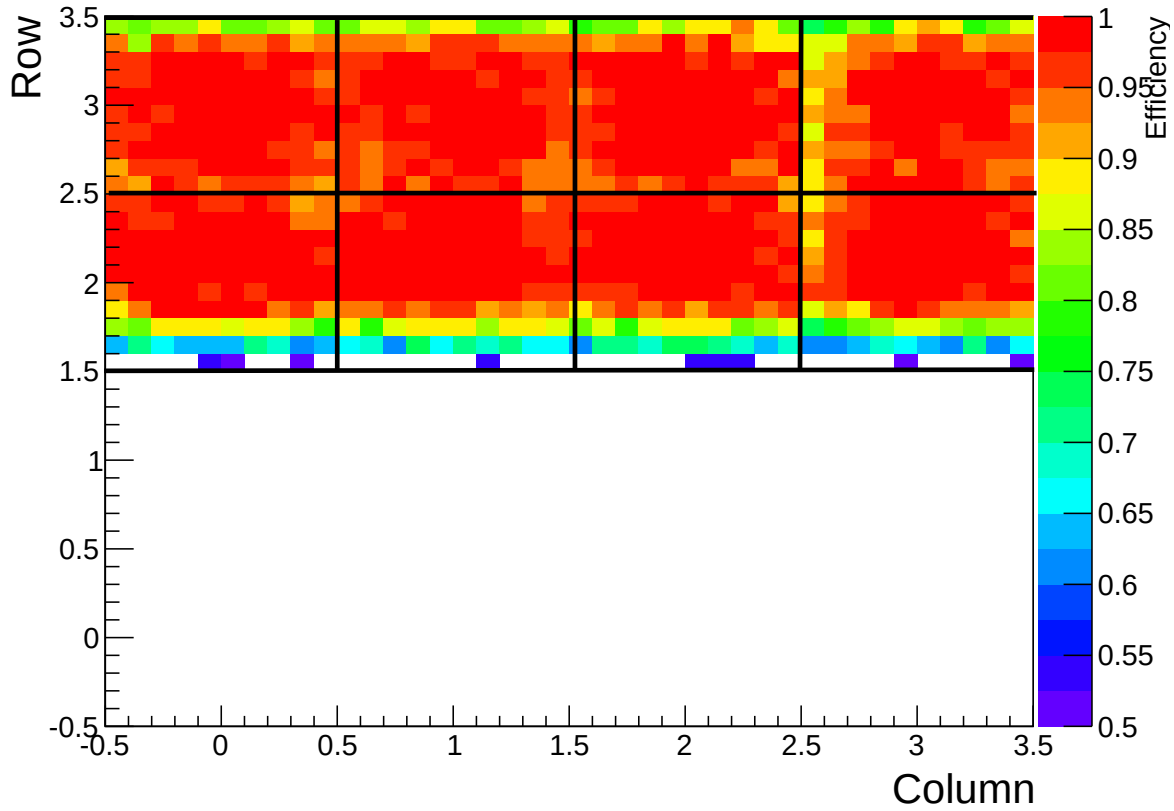

- structure with reduced efficiency at pixel borders
- caused by wrong potential of guard ring

Efficiency with Column Information

hit-track matching using only column information

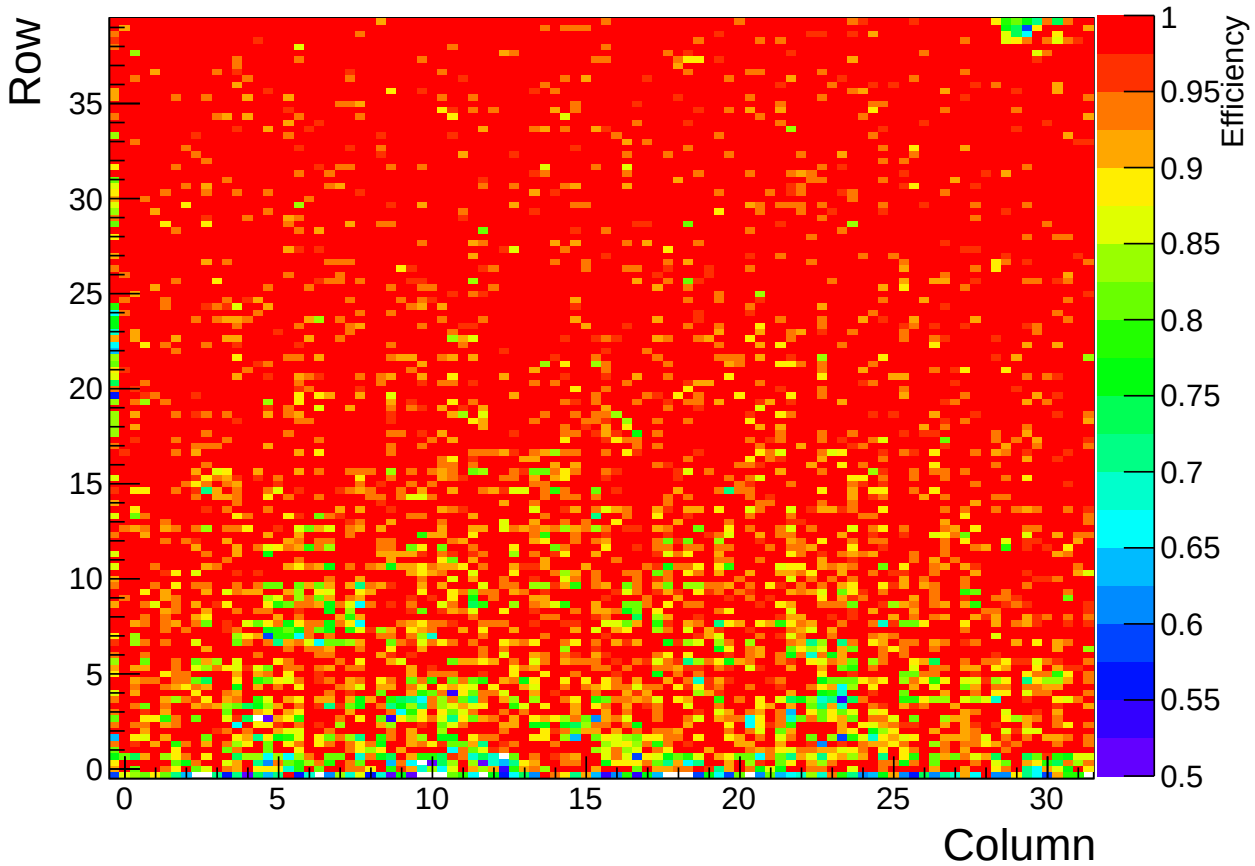

- high efficiency also in broken rows

Efficiency without TDAC tunning

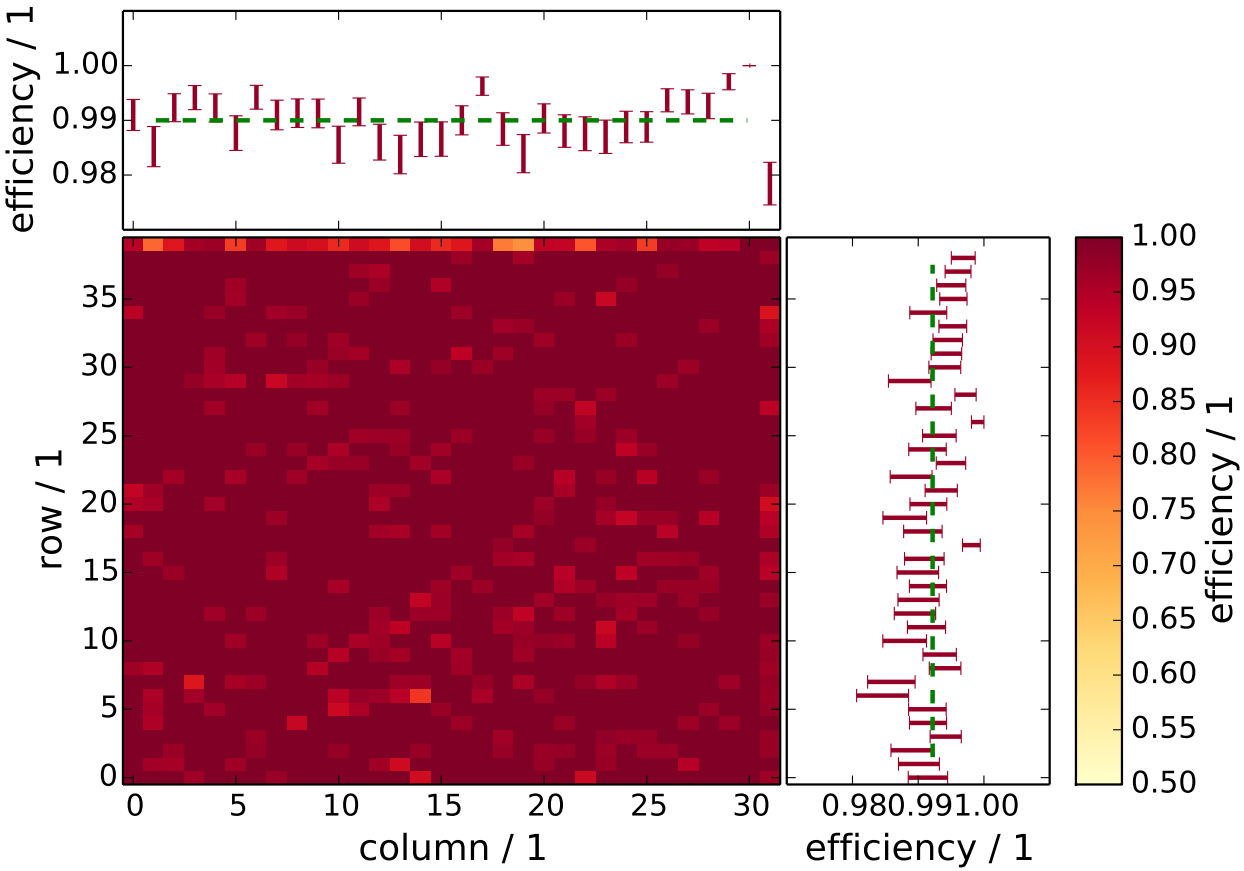

- homogeneous efficiency distribution
- efficiency around 99%

PANDA DAQ

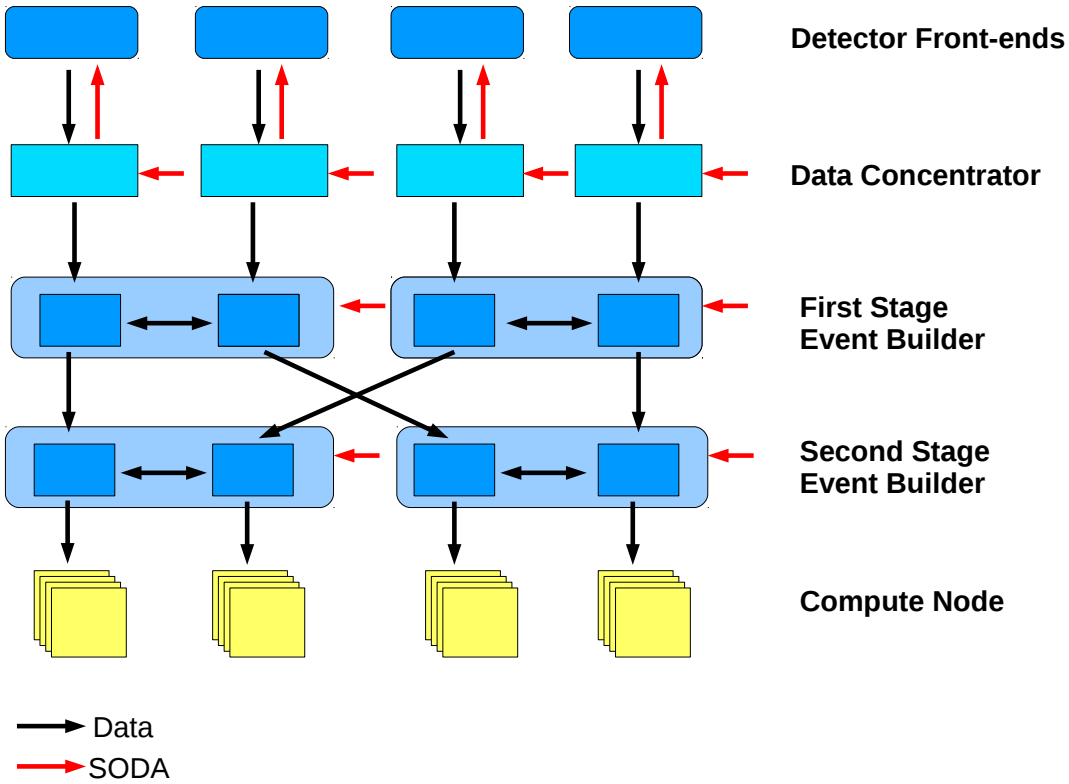

- generation of online trigger
- synchronisation of sub-detectors

Luminosity Detector Frontend Board

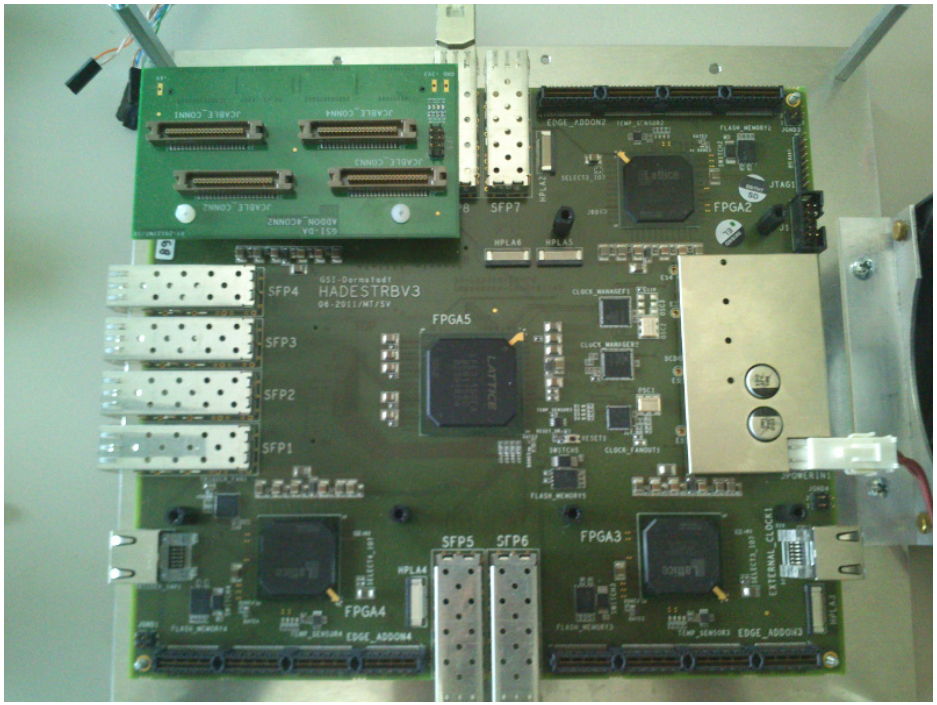

- HADES Trigger and Readout Board
  (M. Traxler et al 2011 JINST 6 C12004)
- 5x Lattice ECP3-150 FPGAs
- main FPGA for UDP/inter FPGA connectivity
- four side FPGAs for sensor I/O

Luminosity DAQ

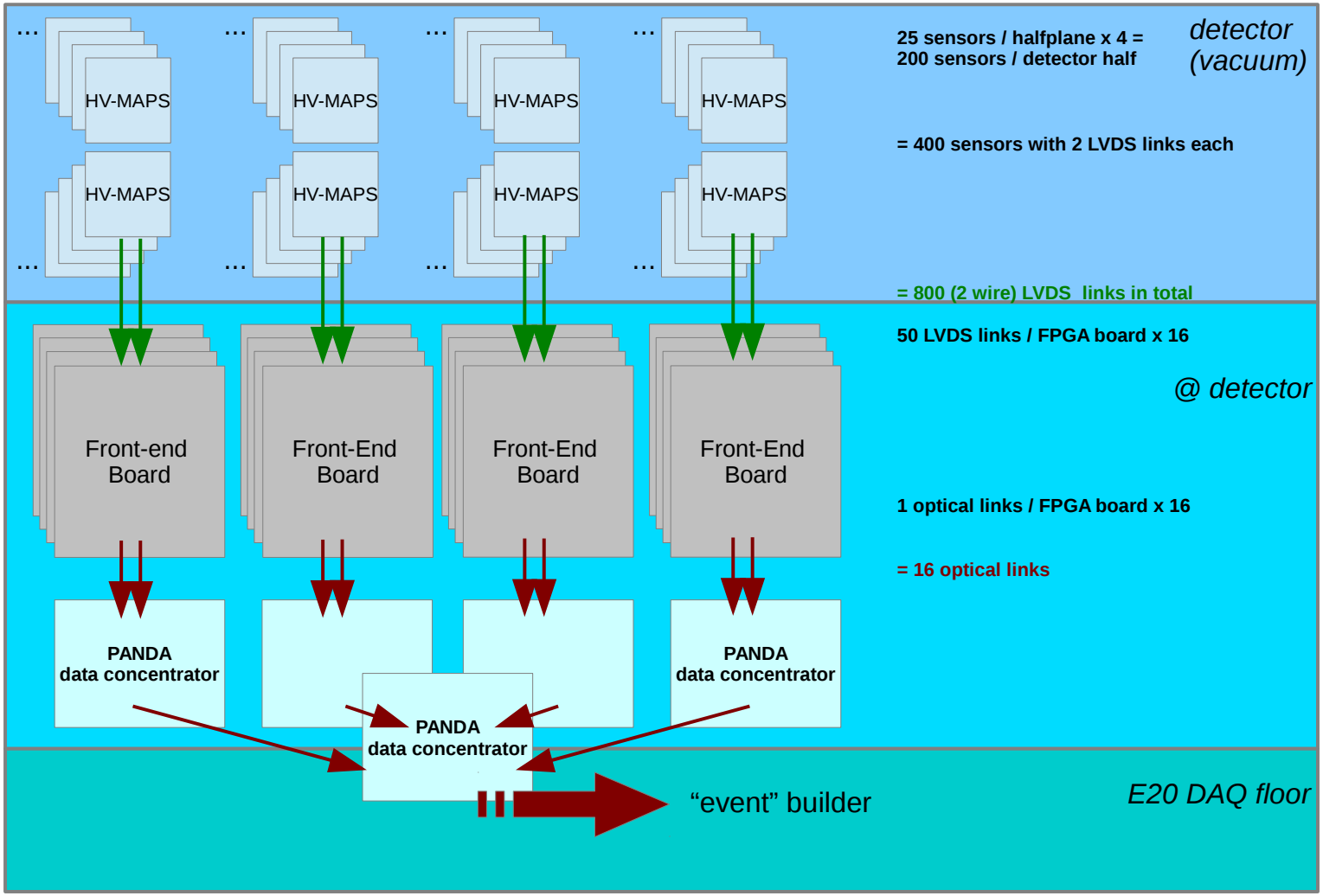

Summary

- test beam in October 2013
- efficiencies look promising
- problem with row address readout in MuPix 4

Outlook

- next MuPix iteration in March
  - correction of row readout
  - additional amplifier-stage $\Rightarrow$ improved signal-to-noise
  - better discriminator

Thank you for your attention!

Backup Slides

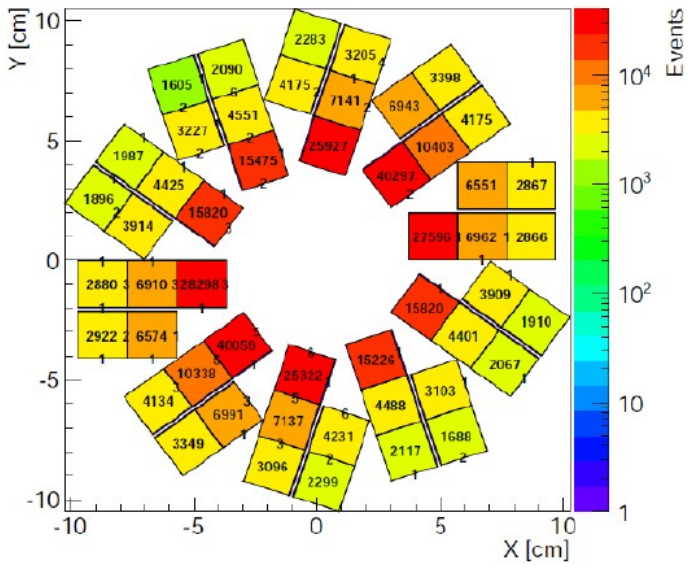

Abbildung 5.2: Ereignisraten auf der ersten Detektorebene bei $1.5\frac{GeV}{c}$ Strahlimpuls.

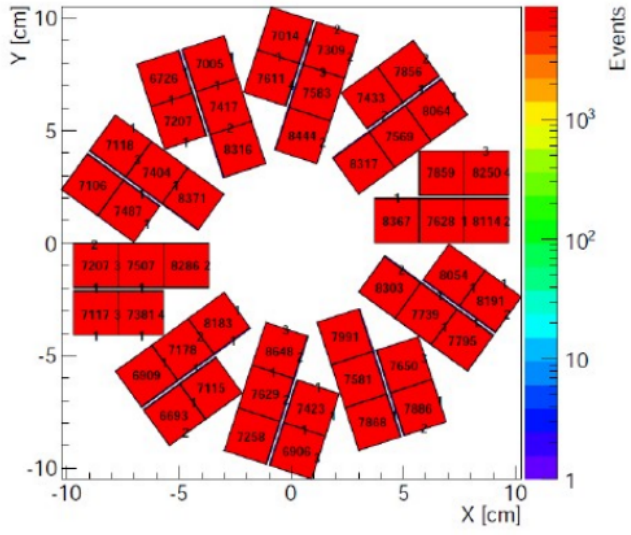

Abbildung 5.4: Ereignisraten auf der ersten Detektorebene bei $15\frac{GeV}{c}$ Strahlimpuls.

Antiprotonen Impuls $[\frac{GeV}{c}]$	Benutzter Wert	Rate [kHz]
1.5	Sensor 1	183, 2
1.5	Sensor 3	19, 0
15.0	Sensor 1	40, 0

Radiation doses

Ebene	Seite	Sensor	Dosis [Gy 0.795s]	Dosis [Gy a]
1	vorn	3	$6.64 \cdot 10^{-5}$	1317
1	vorn	1	$38.5 \cdot 10^{-5}$	7636
4	hinten	3	$16.4 \cdot 10^{-5}$	3253
4	hinten	1	$159.4 \cdot 10^{-5}$	31615

Tabelle 4.4: Maximal deponierte Dosis bei $1.5\frac{GeV}{c}$ aus der Simulation und extrapolierte Dosis für ein Betriebsjahr.

Ebene	Seite	Sensor	Dosis [Gy 1.6s]	Dosis [Gy a]
1	vorn	3	$6.98 \cdot 10^{-5}$	688
1	vorn	1	$7.19 \cdot 10^{-5}$	709
4	hinten	3	$20.2 \cdot 10^{-5}$	1990
4	hinten	1	$18.7 \cdot 10^{-5}$	1843

Tabelle 4.6: Maximal deponierte Dosis bei $15\frac{GeV}{c}$ aus der Simulation und extrapolierte Dosis für ein Betriebsjahr.

In additon ~250Hz neutrons/sensor @ 15GeV/c
→ **should not be an issue.**